

# Acid-Catalyzed $\alpha$ -O-4 Aryl-Ether Cleavage Mechanisms in (Aqueous) $\gamma$ -Valerolactone: Catalytic Depolymerization Reactions of Lignin Model Compound During Organosolv Pretreatment

Edita Jasiukaitytė-Grojzdek, Matej Huš, Miha Grilc,\* and Blaž Likozar\*

Cite This: <https://dx.doi.org/10.1021/acssuschemeng.0c06099>

Read Online

ACCESS |



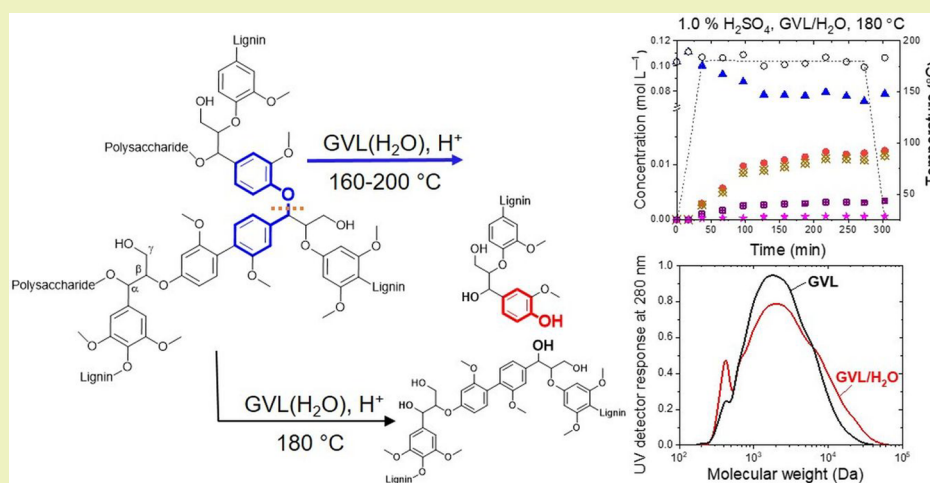
Metrics &amp; More



Article Recommendations



Supporting Information



**ABSTRACT:** In this study, acidolysis of benzyl phenyl ether (BPE), being a representative lignin model compound with the  $\alpha$ -O-4 linkage, was examined in  $\gamma$ -valerolactone (GVL) and a GVL/water mixture, each time acidified with sulfuric acid. The product distribution was strongly affected by water used as a cosolvent, which was found to be advantageous by inhibiting the formation of larger structures and introducing reactive OH groups instead. The experimental results indicate the GVL/water ratio as an important parameter to attain an optimal hydrolytic  $\alpha$ -ether bond cleavage. Differences between the organosolv lignins (molecular weight distribution, OH group content, and structural features with reaction time), isolated under moderate reaction conditions, supported the findings obtained using BPE. A beneficial effect of the added water is reflected in the higher aliphatic OH group content and less intact structure. Analysis of the reaction mechanism represents an initial step toward kinetics and structure–activity correlation of biorefining industrial resources.

**KEYWORDS:** Organosolv,  $\alpha$ -O-4, Ether bond, Lignin isolation,  $\gamma$ -Valerolactone

## INTRODUCTION

Environmental issues regarding climate change and the looming depletion of fossil fuels are the main driving forces encouraging us to transform into a biobased society. This can be achieved by developing new, alternative, and sustainable procedures of producing replacements for petroleum-based products. Lignocellulosic (LC) biomass has been recognized as a suitable renewable material with a high potential for the conversion into various chemicals<sup>1</sup> as well as precursors for polymer synthesis.<sup>2</sup> Lignin is one of the major components of LC biomass. It has an aromatic, three-dimensional, highly functionalized network and has been a subject of numerous studies on producing chemicals, especially bioaromatics.<sup>3–5</sup>

Overall, the efficiency of LC biomass valorization is strongly dependent on the fractionation procedure used to separate the

initial material into its three main constituent parts: cellulose, hemicellulose, and lignin. Further conversion imposes partial structural changes of the isolated macromolecule. It could eventually be tailored within fractionation depending on the type of the selected depolymerization/upgrading process.<sup>6–8</sup> In general, the content of  $\beta$ -O-4 bonds in lignin is one of the key

**Received:** August 19, 2020

**Revised:** October 12, 2020

parameters of its suitability for further conversion into value-added chemicals.

The fractionation of LC biomass using the organosolv process in (aqueous) organic solvents has been recognized as an environmentally friendly process which yields lignin rich in ether bonds.<sup>5</sup> However, a regular organosolv pulping system using aqueous ethanol typically requires high pressures, which is considered an important disadvantage due to high equipment costs. The high pressure drawback could be solved by dissolving lignin in  $\gamma$ -valerolactone (GVL). It remains stable in acidic systems even at high temperatures; has a high boiling point (207 °C); and is nontoxic, nonvolatile, and water-miscible.<sup>9,10</sup> Moreover, GVL is a green, biomass-derived solvent and, coupled with water in a binary mixture, hydrolyses hemicellulose, thus dissolving lignin while leaving cellulose intact. The recovery of GVL is also not complicated. As water and GVL do not form an azeotrope, water is easily removed by distillation. This makes recycling GVL a less-energy demanding process than recovering ethanol.<sup>11</sup> GVL from a carbohydrate-rich water solution could be also separated by adding NaCl (salting out) or extracting with CO<sub>2</sub>. This type of GVL recovery was employed by Luterbacher et al. after isolating soluble carbohydrates from LC biomass using GVL/water and dilute acid (0.05 wt % of H<sub>2</sub>SO<sub>4</sub>) with high yields (70–90%).<sup>9</sup>

Based on the beneficial properties of the GVL/water mixture for LC biomass decomposition, it had been proposed as a reaction medium for wood fractionation to recover intact cellulose (paper-grade or dissolving pulps), uniform sugar components from hemicellulose, and pure lignin.<sup>12</sup> Lignin in the GVL/water solvent system is isolated under acid-free conditions or mild acidic conditions depending on the target products.<sup>9,12</sup> The highest expected lignin removal from the pretreated substrates is 80–90%,<sup>13,14</sup> while the yields of the recovered lignin by precipitation are reported with a more modest ~40%.<sup>15,16</sup> However, by employing a two-step lignin precipitation with vacuum distillation, a yield of more than 90% could be attained.<sup>13</sup> The chemistry of GVL pulping and the corresponding reaction pathway have not been fully investigated yet. Until now, the rate of the hydrolysis of glycosidic bonds in an acidic GVL/water system was investigated using mono- and disaccharides as model compounds. Higher reaction rates were reported for biomass hydrolysis.<sup>17</sup> Hydrothermal decomposition of cellobiose in acid-free GVL/water was investigated by Song et al. The authors demonstrated GVL/water to be a promising reaction medium for the recovery of glucose even under acid-free conditions, which is evidently due to the more pronounced hydrolysis and suppressed isomerization reaction.<sup>18</sup>

While the mechanism of hydrothermal sugar decomposition in (acidic) GVL/water is clarified, the effect of an acidic GVL-based reaction medium on the structure of lignin remains uncertain. Although pure “native-like” lignin was obtained after acid-free GVL/water fractionation,<sup>6</sup> it is essential to understand the mechanism of the ether bond cleavage and the effects of operating conditions in an acid-catalyzed system to eventually optimize/tune its properties in terms of the functionality and/or molecular weight of isolated lignin.

In this study, we investigated the cleavage of the aryl-ether bond in acidic GVL. The reaction mechanism and the effects of temperature, acidity, water addition, and solvent acidity were studied. The effect of the process conditions (including the amount of water used as a cosolvent) on the progression of

the reaction and the product distribution was studied. In the organosolv pulping, lignin-carbohydrate and  $\alpha$ -O-4 bonds in the lignin macromolecule are broken predominantly,<sup>19</sup> which is mimicked by a clever choice of the model compound in this study. Benzyl phenyl ether (BPE) has been used in numerous papers to examine mechanisms of the catalytic  $\alpha$ -ether bond scission in aqueous and apolar solvents,<sup>20–22</sup> supercritical methanol, and supercritical water<sup>23</sup> as a representative of the most labile C–O bond in lignin (bond dissociation energy 215 kJ mol<sup>-1</sup>).<sup>24</sup> Furthermore,  $\alpha$ -O-4 is a characteristic lignin-carbohydrate bond which is necessary to cleave to release lignin from the LC biomass.<sup>25</sup> Accordingly, we use benzyl phenyl ether as an  $\alpha$ -O-4 model compound to study the cleavage of aryl-ether bonds in the lignin structure.

The acidolysis of benzyl phenyl ether, itself an important model compound containing the  $\alpha$ -O-4 linkage, has been investigated in GVL and in 75 vol % GVL/water with sulfuric acid. We seek to understand the effect of GVL in the organosolv process on the extent of the C–O bond cleavage in aqueous and nonaqueous reaction media. Additionally, the influence of the reaction media acidity and temperature on the product distribution (revealing the conversion and selectivity of the existing reactions) over time was studied. Consequently, examination of further model compounds, representing the most frequent linkages in lignin, would allow for the development of a microkinetic model, explicitly taking into account the characteristics of the reaction media and describing the process as a sequence of elementary reactions, which was beyond the scope of this research. The study primarily focuses on drawing the correlation between the model compound and the real sample of lignin. Therefore, the effect of the reaction medium on the isolated organosolv lignin structure was investigated.

## EXPERIMENTAL SECTION

**Materials.** All the chemicals, gases, solvents, and external calibration standards were of reagent grade and were used as purchased without further purification. The suppliers, CAS numbers, and purity of chemicals are provided in the [Supporting Information](#).

**Experiments.** The experiments were performed in six parallel slurry reactors (Amar Equipment Pvt. Ltd., Mumbai, India), consisting of vessels with a volume of 250 mL, equipped with magnetically driven Rushton turbine impellers. The experiments performed are summarized in [Table S1](#). Details are provided in the [Supporting Information](#).

The model compound benzyl phenyl ether (BPE, 1.7 g) was dissolved in GVL or 75 vol % GVL/water (89.5 mL of GVL and 29.5 mL water) in a ratio of 1:70 (w/v). The experiments were performed in the temperature range of 160–200 °C with varying H<sub>2</sub>SO<sub>4</sub> amount (0.025–0.075 g) in the form of a 2 M solution for 1 g of the model compound.

The liquid samples from the reactor vessel were taken in 30 min intervals after the reaction mixture reached the set temperature. Two more samples were withdrawn at room temperature and halfway through the heat-up ramp. Overall, 11 samples of 1 mL were collected for each experiment.

**GC-MS Analysis.** The samples were examined using gas chromatography coupled with mass spectrometry (GC-MS; 2010 Ultra, Shimadzu, Kyoto, Japan) with an added flame ionization detector (FID), equipped with a Zebtron ZB-5 (Phenomenex, Torrance, CA, USA) 60 m  $\times$  0.25 mm  $\times$  0.25  $\mu$ m capillary column. The concentration of the majority of identified products in the samples was evaluated based on the calibration curves for the known concentrations of the external standards, while response factors of a few more complex identified products (representing less than 10% of total FID peak area) had to be determined by the group contribution

method, involving the regression analysis based on the response factor of 27 different aromatic compounds. The quantitative GC-MS/FID data reported in this study are the averages of three trials. The maximum standard error for concentrations was  $7.2 \times 10^{-4}$  mol L<sup>-1</sup>, while the maximum standard deviation was  $1.2 \times 10^{-3}$  mol L<sup>-1</sup>. For more details, see the [Supporting Information](#).

Conversion ( $X_{\text{BPE}}$ ) of BPE (in %) was calculated according to eq 1.

$$X_{\text{BPE}} = \left( \frac{C_{\text{BPE}}(t=0) - C_{\text{BPE}}(t)}{C_{\text{BPE}}(t=0)} \right) \times 100 \quad (1)$$

where  $C_{\text{BPE}}(t=0)$  stands for the initial BPE concentration, while  $C_{\text{BPE}}(t)$  represents the concentration of BPE at a given time.

In order to retain the clarity of the results, all concentrations ( $C_i$ ) of reactants, intermediates, and products were normalized (asterisk denotes normalization) per number of aromatic rings ( $N_i$ ) in a compound  $i$  ( $i$  is their number).

$$C_i^* = C_i \times N_i \quad (2)$$

Molar balance per aromatic ring was followed, as this stable motif was conserved throughout the reactions.

$$C_{\text{tot}}^* = \sum_i C_i^* \quad (3)$$

**Lignin Extraction.** Organosolv lignin was isolated from beech tree sawdust (3 g, 24 mesh, dried at 105 °C for 24 h) with GVL, 75 vol % GVL/water (22.5 mL of GVL and 7.5 mL of water) in a ratio of 1:10 (w/v). To catalyze the reaction, 0.5% of H<sub>2</sub>SO<sub>4</sub> based on dry feedstock mass was added to the reaction mixture. The extraction was performed in a Parr reactor system (Parr 5000) at 180 °C over different time intervals. Each reactor was flushed twice and pressurized with nitrogen up to 1 MPa. The experiments were carried out in a batch regime with an agitation speed of 600 min<sup>-1</sup>. The reaction was quenched by dipping the reactor in an ice bath. The solid particles were filtered out and rinsed with 100 mL of hot (80 °C) water. The remaining particles were dried at 105 °C for 48 h. The organosolv lignin was precipitated by adding distilled water in a 10-fold excess. The precipitate was collected upon a 10 min centrifugation at 4500 rpm, repeatedly washed with distilled water, and freeze-dried. The yield of residue and of the isolated lignin (%) was calculated with respect to the starting beech wood according to eq 4:

$$\text{Yield (\%)} = \left( \frac{W_t}{W_0} \right) \times 100 \quad (4)$$

where  $W_t$  stands for the weight of the remaining residue or the isolated lignin and  $W_0$  is the weight of the starting beech wood.

**2D HSQC and <sup>31</sup>P NMR Analysis.** 2D heteronuclear single quantum coherence (HSQC) NMR spectra were recorded using a Bruker AVANCE NEO 600 MHz NMR spectrometer equipped with BBFO probe following the protocol reported by Tran et al.<sup>26</sup> Approximately 85 mg of lignin sample was dissolved in 0.6 mL of DMSO-*d*<sub>6</sub>, which was also used as an internal chemical shift reference point ( $\delta_{\text{C}}$  40.1;  $\delta_{\text{H}}$  2.50 ppm). HSQC spectra analysis, assignment of the different lignin cross-signals, and calculations were made following the reported procedure.<sup>27</sup>

Quantitative <sup>31</sup>P NMR experiments were carried out precisely following the protocol reported elsewhere.<sup>28</sup> The measurements were conducted in CDCl<sub>3</sub>/pyridine 1:1.6 mixture at 25 °C, and *N*-hydroxy-5-norbornene-2,3-dicarboxylic acid imide (NHND) was used as an internal standard. Prior to the analysis, lignin samples were derivatized using 2-chloro-4,4,5,5-tetramethyl-1,2,3-dioxaphospholane (TMDP). Three parallel <sup>31</sup>P NMR measurements were performed for each sample, and the averages are reported in this work. The maximum standard deviation of presented results was  $2 \times 10^{-2}$  mmol g<sup>-1</sup>, while the maximum standard error was  $1 \times 10^{-2}$  mmol g<sup>-1</sup>.

**Size-Exclusion Chromatography (SEC).** Prior to the analyses, the lignin samples were acetylated with pyridine/acetic anhydride

according to the procedure reported elsewhere.<sup>29</sup> SEC was performed on a size-exclusion chromatographic system (Ultimate 3000, Thermo Fisher Scientific, Massachusetts, US) equipped with a UV detector set at 280 nm and a PLgel 5 μm MIXED D 7.5 × 300 mm column with THF as an eluent at a flow rate of 1 cm<sup>3</sup> min<sup>-1</sup>. Calibration was made with polystyrene standards (Polymer Standards Service; PSS) with molecular weights in the range from 127 kDa to 672 Da. The chromatographic data were processed with the PSS WinGPC Unity software.

## RESULTS AND DISCUSSION

While the mechanism of initial lignin depolymerization during organosolv pulping with alcohols had been extensively studied, the chemistry of lignin conversions during the GVL-based pulping process remains unclear. Lignin depolymerization during alcohol-based pulping is mainly a result of the α-ether bond cleavage, which is the rate-determining step. Due to a higher bond dissociation energy of β-ethers (BDE(α-O-4) = 215 kJ mol<sup>-1</sup>; BDE(β-O-4) = 290 kJ mol<sup>-1</sup>),<sup>24</sup> which implies a higher activation barrier, only a limited amount is cleaved in, for instance, ethanol-based pulping.<sup>30</sup> Sturgeon et al. showed the rate of the β-O-4 cleavage also strongly depends on the presence of side groups, explaining why the observed rate of acidolysis can differ between model compounds and biomass-derived lignin. A neighboring phenolic hydroxyl group can accelerate the reaction rate by 2 orders of magnitude, which is caused by a different stability of the involved intermediates. The β-O-4 linkages are cleaved at the phenolic ends through an ionic mechanism.<sup>31</sup> Noncanonical lignin monomers, such as tricin, can also incorporate in the lignin polymeric structure forming a β-O-4' bond. The average energy of reaction for hemolytic bond cleavage was calculated as 230 kJ mol<sup>-1</sup>, depending on the monomers. While the acylated varieties generally exhibited lower than average values, the differences were not stark.<sup>32</sup> Sangha et al. also calculated reaction enthalpies for dimerization of lignin monomer radicals. Bond dissociation energies are 330-340 kJ mol<sup>-1</sup> for *p*-coumaryl, coniferyl, and sinapyl species.<sup>33</sup> None of these studies accounted for an explicit solvent, which can significantly change the reaction thermodynamics and kinetics.

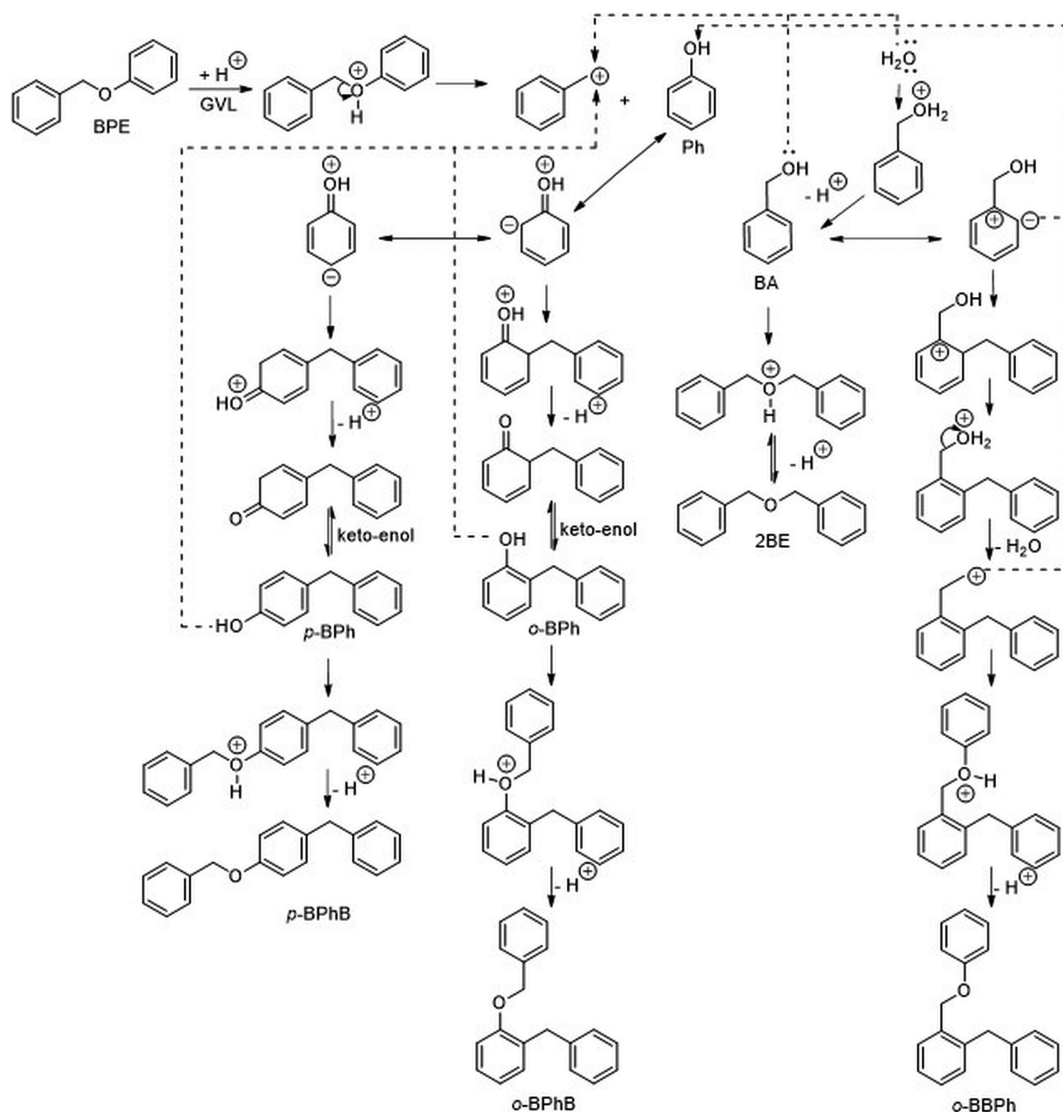
This makes it a more suitable reaction medium for lignocellulosic biomass fractionation, especially when the isolation of β-ether-rich lignin is desired.

A major problem, however, is the additional alkoxylation of lignin, which is caused by the alcohol used. It reduces the reactivity of lignin (i.e., hydroxyl group content). However, this can be overcome by using GVL instead, because it does not act as an external nucleophile as shown in [Scheme 2](#).

Therefore, to elucidate the effect of GVL on the α-O-4 bond cleavage under conditions which are commonly used for ethanol-based pulping, BPE (α-O-4 model compound) was chosen.

**Reaction Mechanism.** In an acid medium, ether hydrolysis usually follows the S<sub>N</sub>1 or S<sub>N</sub>2 mechanism. The faster S<sub>N</sub>1 mechanism is generally the dominant one, except when it would lead to the formation of unstable carbocations (such as primary or secondary alkyl, vinyl, or aryl). With BPE, a stable benzyl carbocation can form.

To propose the mechanism of the α-O-4 bond cleavage in acidified aqueous and nonaqueous GVL, we use the data from our GC-MS analyses. Therein, we identify the following main products: phenol (Ph), benzyl alcohol (BA), 2-benzyl phenol (*o*-BPh), 4-benzyl phenol (*p*-BPh), dibenzyl ether (2BE), 1-benzyl-4-(benzyloxy)benzene (*p*-BPhB), and 1-benzyl-2-

Scheme 1. Proposed Reaction Mechanism of  $\alpha$ -O-4 Bond Cleavage in (Aqueous) GVL

(phenoxymethyl)benzene (*o*-BBPh). When water was added, substantially higher amounts of benzyl alcohol (BA) were formed. In general, we observe that the reaction conditions (i.e., solvent, acidity, and temperature) strongly affected the product distribution.

Under acidic conditions, BPE is first protonated on the ether oxygen atom. Although this reaction proceeds to a small extent ( $pK_b$  for aryl alkyl ethers is around 20), the protonated BPE quickly dissociates via the  $S_N1$  mechanism, yielding a benzyl carbocation and phenol (a converse reaction yielding benzyl alcohol and a phenyl carbocation is not possible on thermodynamic grounds due to the instability of the cation). Pelzer et al.<sup>22</sup> showed that in aqueous solutions phenol and benzyl alcohol form upon overcoming a Gibbs barrier of 145 kJ mol<sup>-1</sup>,<sup>34</sup> while further condensation reactions have lower barriers. They modeled the reaction with implicit solvent and three water molecules.

Under aqueous conditions, the benzyl carbocation reacts with water, yielding (protonated) benzyl alcohol, making this essentially an acid-catalyzed BPE hydrolysis. When water concentration is sufficient, the carbocation might not be

stabilized, but the protonated benzyl alcohol forms immediately,<sup>22</sup> while in pure GVL a carbocation must form.

However, under nonaqueous conditions, the cation can either react with phenol or benzyl alcohol. When phenol and benzyl alcohol react through their oxygen atoms, BPE (no net reaction) or dibenzyl ether form, respectively. However, due to the resonance effect of the OH group, *ortho* and *para* carbon atoms in phenol are also activated (surplus of electron density, depicted by the resonance structures with the negative charge on the carbon atoms in Scheme 1). This allows for a condensation reaction yielding *o*-BPh and *p*-BPh after deprotonation and ketoenol isomerization. Pelzer et al. calculated that the barriers for these condensations are lower than for the initial ether hydrolysis.<sup>22</sup> When the hydroxyl group in BA reacts with the carbocation, 2BE is formed (essentially, this is transesterification).

Even when using nonaqueous GVL, small amounts of water are also introduced in the system with H<sub>2</sub>SO<sub>4</sub>, which is itself an aqueous solution. Consequently, small amounts of BA can form which react with the benzyl carbocation to form 2BE due to the lack of other suitable reactants. In aqueous solution, water preferentially reacts with the carbocations, preventing

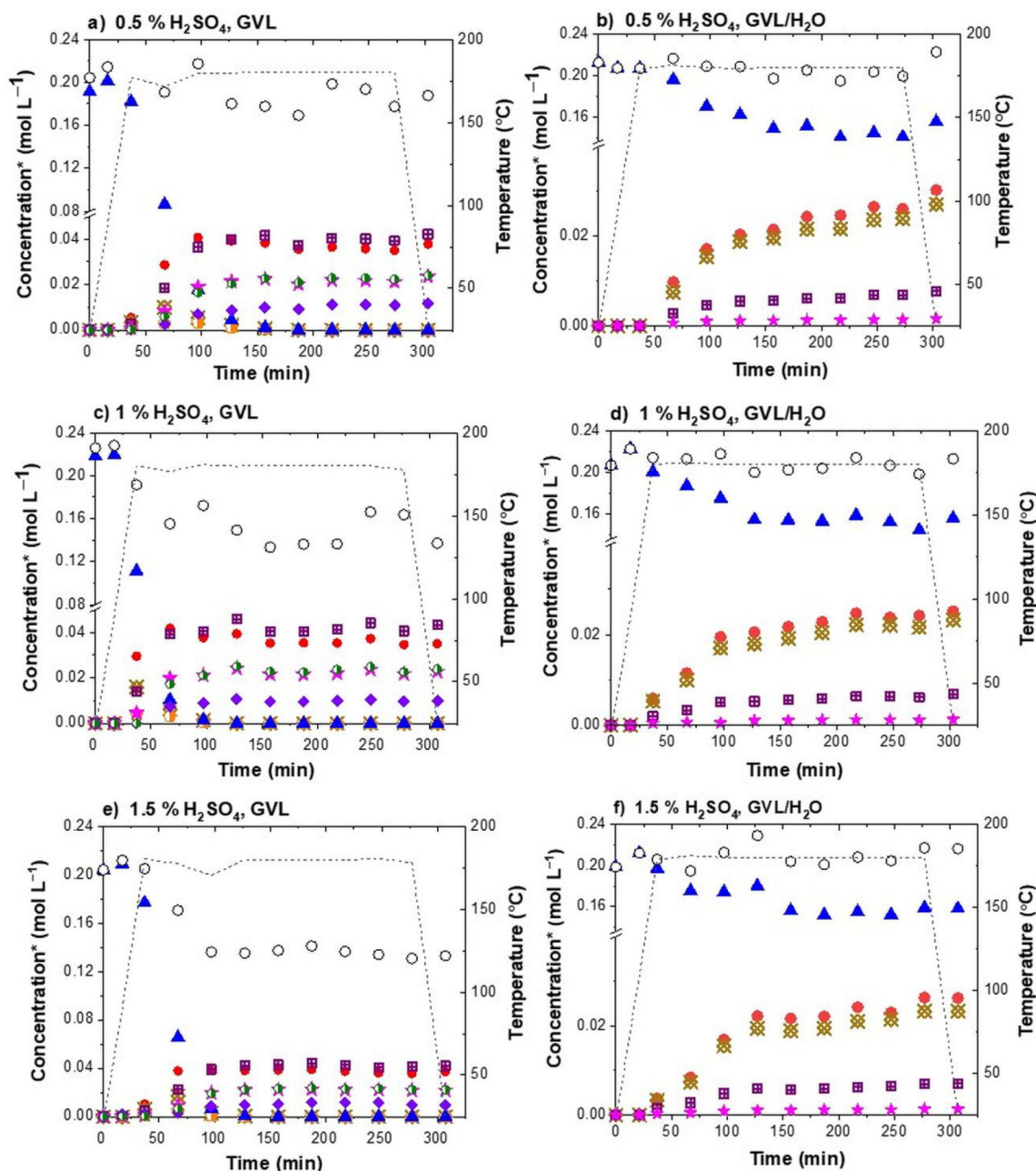


**Figure 1.** Normalized (asterisk denotes concentration normalized per aromatic ring) product distribution during the BPE acidolysis in  $\gamma$ -valerolactone (GVL) or  $\gamma$ -valerolactone/water (GVL/H<sub>2</sub>O) at 180 °C with 0.5% of H<sub>2</sub>SO<sub>4</sub> (a, b), 1.0% of H<sub>2</sub>SO<sub>4</sub> (c, d), and 1.5% of H<sub>2</sub>SO<sub>4</sub> (e, f). Key: blue triangle, benzyl phenyl ether (BPE); red circle, phenol (Ph); brown braid, benzyl alcohol (BA); purple crossed box, 2-benzyl phenol (*o*-BPh); magenta star, 4-benzyl phenol (*p*-BPh); orange half pentagon, dibenzyl ether (2BE); green half octagon, 1-benzyl-4-(benzyloxy)benzene (*p*-BPhB); violet diamond, 1-benzyl-2-(phenoxy)methylbenzene (*o*-BBPh); open circle, molar balance (per aromatic ring, according to eq 3); ---, temperature.

the formation of 2BE. As discussed below, the reaction in aqueous media is slower.

The hydroxyl group of *p*-BPh and *o*-BPh can react with the benzyl carbocation, forming (protonated) *p*-BPhB and *o*-BPhB, respectively. In BA, the *ortho* position is weakly activated and can also directly attack the carbocation (the activation is weaker than in phenol). This transiently yields (2-benzylphenyl)methanol (BPhM), which was not detected experimentally. However, upon protonation, BPhM dissociates via the S<sub>N</sub>1 mechanism to give the (2-benzyl)benzyl carbocation, which can react with the activated *ortho* position

in BA, yielding (protonated) *o*-BBPh, which we *did* detect. The whole mechanism is depicted in Scheme 1.

**The Effect of Water.** Delignification of LC biomass is a complex procedure involving an initial lignin release from the cellular and intercellular material in lignocellulose by hydrolytic ether bond cleavage in a lignin-carbohydrate complex or between lignin fragments. For this reason, water is typically used for the organosolv-type LC biomass fractionation along with organic solvents.<sup>35,36</sup> At elevated temperatures, water facilitates the cleavage of the acetyl group in hemicellulose, forming acetic acid. This accordingly creates the necessary

acidic conditions for inducing the ether bond cleavage and releasing lignin from the biomatrix.<sup>37</sup> To ensure an efficient isolation of lignin, the equilibrium between the macromolecule release and dissolution must be achieved. According to the Hildebrand solubility parameter theory, the optimal solubility of beech wood lignin should be reached in 92–96 wt % GVL. However, an insufficient hydrolytic ether bond cleavage limits the extent of delignification in this case, removing only minor amounts of lignin. An optimal hydrolytic ether bond cleavage and, accordingly, biomass delignification were achieved using 50–60 wt % GVL.<sup>12</sup>

Hence, in our work, the effectiveness of 75 wt % GVL (average concentration) in the hydrolytic ether bond cleavage in BPE (an  $\alpha$ -O-4 model compound) was tested. In addition, the effects of the reaction temperature and acidity of the reaction media were investigated with the emphasis on the preservation of functional (hydroxyl) groups.

In order to determine the effect of water, the experiments were carried out in both aqueous and nonaqueous GVL. GVL itself is not a nucleophile and remains inert through the reaction. As discussed in the previous section and depicted in Scheme 1, the benzyl carbocation, produced after the protonation-induced  $\alpha$ -ether bond cleavage, tends to react with the other reactive species forming dimers (*p*-BPh, 2BE, *o*-BPh) and trimers (*p*-BPhB, *o*-BPhB, *o*-BBPh).

When water is introduced into the system, the benzyl carbocation reacts mostly with water ( $S_N1$  reaction). This reduces the amount of the reaction intermediates formed, as water is a better nucleophile than (activated) phenol, let alone benzyl alcohol. Thus, BA is the main product formed from BPE in the presence of water.

Analyzing the BA concentration profiles, the starkest difference is seen when comparing the experiments performed with 1% of  $H_2SO_4$  at 180 °C (runs 3, 4), shown in Figure 1c and d. In the case of nonaqueous GVL, the highest BA concentration is detected after 40 min when the temperature plateau is reached. The formation of the BA is the result of the reaction with the water from the  $H_2SO_4$  solution. As soon as all water is consumed, that is 10 min after reaching the temperature plateau at 180 °C, the concentration of BA decreases due to the formation of trimeric *o*-BBPh.

When performing the reaction in aqueous GVL, BA is continuously produced along with phenol, along with minor amounts of *o*-BPh and *p*-BPh.

At the same time, the reaction rate is considerably lower in the presence of water, which is most evident when comparing the BPE concentration profiles in Figure 1c and d. In addition, Figure 2 demonstrates that a virtually complete conversion of BPE in nonaqueous GVL is achieved within 2 h, while in aqueous GVL the conversion levels off at approximately 25%.

The lower activity in aqueous media as opposed to nonaqueous GVL can be explained two-fold. It has previously been observed that the presence of water decreases the cleavage activity, for instance, in deep eutectic solvents. Water not only dilutes the solution (which is not the case in our case as acid concentration is maintained constant) but retards the reaction progress because an ether bond cleavage requires initial protonation, for which water can also act as a reagent.<sup>38</sup> Indeed water is preferentially protonated in comparison with BPE ( $pK_b$  of water and alkyl aryl ethers is 15.7 and ~20, respectively). This means that introducing water to the system lowers the activity of  $H_2SO_4$  (aqueous dilution).

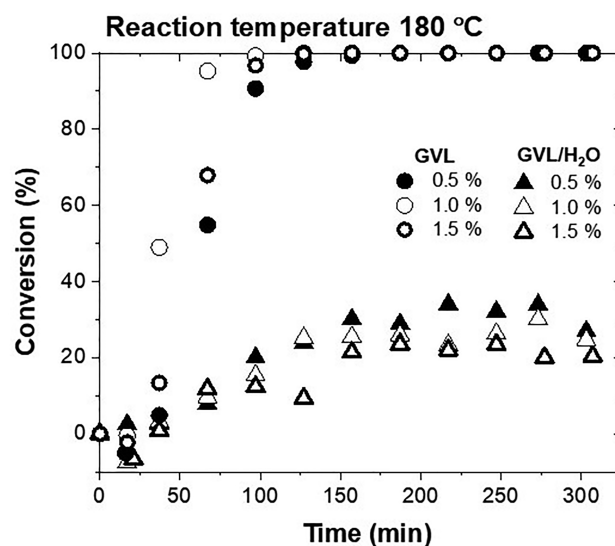


**Figure 2.** Conversion of benzyl phenyl ether (BPE) as a function of time in  $\gamma$ -valerolactone (GVL) and 75 vol %  $\gamma$ -valerolactone/water (GVL/ $H_2O$ ) at 180 °C with 0.5%, 1.0%, and 1.5% of  $H_2SO_4$ .

A second possible consideration is the strong hydrogen bonding by water molecules, which bind to BPE and partially shield it from reacting. This is the controversial iceberg model<sup>39</sup> of water immobilization<sup>40</sup> near hydrophobic solutes, which according to simulations is small.<sup>41,42</sup> This is, in essence, the entropic origin of the hydrophobic effect.<sup>43</sup>

An efficient isolation of lignin with a less intact structure is still challenging. Overall lignin reactivity, mainly governed by its hydroxyl group content, depends on the severity of the structural changes in the biopolymer molecule. During the LC biomass fractionation, lignin undergoes an initial depolymerization which, depending on the conditions, is followed by alkoxylation reactions and/or condensation of the reactive moieties emerging after the cleavage of the interunit bonding. To maintain lignin reactivity, the aliphatic and phenolic hydroxyl groups need to be preserved. In terms of phenolic hydroxyl groups, this could be achieved by performing the fractionation in an inert solvent and introducing water as an external nucleophile to react with benzyl carbocation-type species. This would generate hydroxyl groups instead of initiating the formation of new undesirable C–C bonds.

For the implementation of this approach, GVL/water mixtures for lignin isolation show great potential. It is reasonable to expect an increase in the reaction rate when reducing the water content in the mixture, while still avoiding the formation of larger molecules as in nonaqueous GVL (Scheme 1).

**The Effect of Acidity.** The effect of the acidity of the reaction medium on the  $\alpha$ -O-4 bond scission in (aqueous) GVL was evaluated by performing experiments at 180 °C with 0.5%, 1.0%, and 1.5% of  $H_2SO_4$  (runs 1–6). The distribution of the identified products is shown in Figure 1. The concentration profiles are analogous in both solvents (GVL and GVL/ $H_2O$ ), implying a negligible acidity effect. This hints at the fact that the rate-determining step is not the protonation of BPE itself but the  $S_N1$ -type formation of the carbocation ( $\alpha$ -O-4 bond cleavage). This is observed in nonaqueous and aqueous environments. The catalysis with 1.5% of  $H_2SO_4$  in GVL, however, promotes the emergence of byproducts with

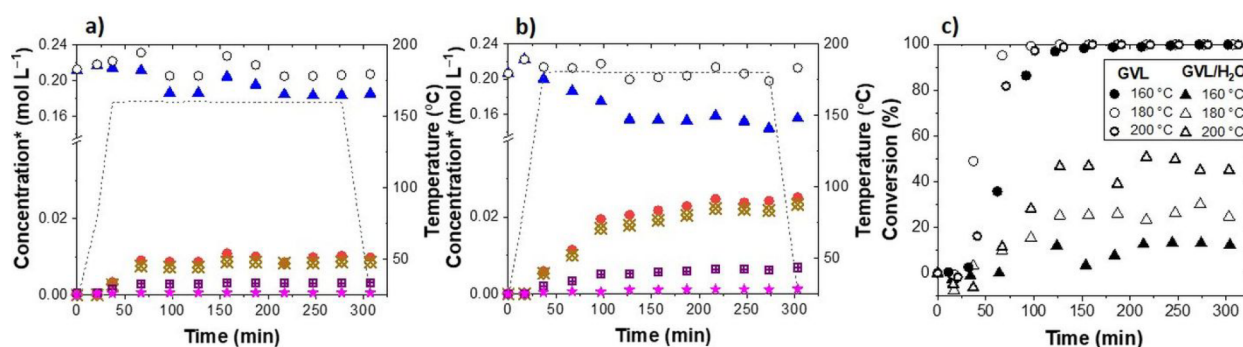


**Figure 3.** Normalized (asterisk denotes concentration normalized per aromatic ring) product distribution during the BPE acidolysis in  $\gamma$ -valerolactone/water (GVL/ $\text{H}_2\text{O}$ ) with 1% of  $\text{H}_2\text{SO}_4$  at 160 °C (a) and 180 °C (b). BPE conversion over the reaction time at 160 °C, 180 °C, and 200 °C in GVL and GVL/ $\text{H}_2\text{O}$  (c). Key: blue triangle, ether (BPE); red circle, phenol (Ph); brown braid, benzyl alcohol (BA); purple crossed box, 2-benzyl phenol (*o*-BPh); magenta star, 4-benzyl phenol (*p*-BPh); open circle, molar balance (per aromatic ring, according to eq 3); ---, temperature.

**Table 1. Lignin Isolation in  $\gamma$ -Valerolactone (GVL) and  $\gamma$ -Valerolactone/Water (75 vol % GVL/ $\text{H}_2\text{O}$ ) with 0.5% of  $\text{H}_2\text{SO}_4$  at 180 °C: Yields of Residue and Lignin, SEC, and Elemental (CHNS) Analysis of Lignins**

exp.	solvent	reaction time [min]	residue [%]	lignin yield <sup>a</sup> [%]	average $M_w$ [Da]	average $M_n$ [Da]	element amount [wt%] <sup>b</sup>			
							C	O	H	N
1	GVL	30	71.6	31.9	3750	1530	61.02	32.68	6.22	0.08
2	GVL	60	75.2	25.4	3500	1460				
3	GVL	120	67.8	32.7	3600	1420	62.39	31.25	6.27	0.09
4	GVL/ $\text{H}_2\text{O}$	120	60.1	51.1	4900	1390	61.19	32.36	6.29	0.16
5	GVL/ $\text{H}_2\text{O}$	180	57.0	60.0	4300	1330				
6	GVL/ $\text{H}_2\text{O}$	240	54.5	65.7	4200	1320	62.5	31.14	6.19	0.17

<sup>a</sup>Initial lignin content in beech wood is considered to be 24.4 wt %. <sup>b</sup>Elemental analysis of lignin samples was performed using a vario EL cube analyzer (Elementar, Hanau, Germany); the presented values are averages of four measurements.

larger structures, which due to the limited volatility are inefficiently detected and, quantified with GC-MS, lowers the molar balance. This experiment accordingly confirms that  $\text{H}_2\text{SO}_4$  in high concentrations intensifies undesirable side reactions.

**The Effect of Temperature.** The effect of temperature on the  $\alpha$ -O-4 bond scission in (aqueous) GVL was tested by running the reaction at 160, 180, and 200 °C (runs 7, 3, 9, 8, 4, 10), acidified with 1%  $\text{H}_2\text{SO}_4$ . Figure 3a and b show the product distribution in aqueous GVL at 160 and 180 °C, while Figure 3c shows the conversion of BPE in (non)aqueous GVL as a function of time. The temperature effect is most evident from the BPE, Ph, and BA concentration profiles.

The temperature rise from 160 to 200 °C markedly increased the rate of the  $\alpha$ -O-4 bond scission and increased the conversion of BPE in aqueous GVL from approximately 10% to 50%. The product distribution was also affected. However, in nonaqueous GVL, only negligible differences among the experiments were observed. Nearly complete reactant conversion was achieved after 100 min at 180 and 200 °C, and after 150 min at 160 °C.

The concentration profiles of the reaction products display a similar pattern. For example, the concentrations of Ph and BA in aqueous GVL remain comparable and show a corresponding increase while raising the temperature. Analogous concentration profiles are obtained even during the highly intense  $\alpha$ -ether acidolysis in GVL. Here, for instance, equivalent BA and *o*-BBPh (BA derivative) concentrations at 160, 180, and 200 °C are obtained after 150, 70, and 60 min, respectively (Figure S1 in the Supporting Information), showing that while the

reaction rate changes, product selectivity is independent of the reaction temperature.

**The Effect of Solvent on Lignin.** On the basis of the results for the model compound, the effect of both solvents (GVL and aqueous GVL) was investigated in the processing of lignin. In particular, beech wood lignin was isolated with GVL and 75 vol % GVL/ $\text{H}_2\text{O}$  under optimal conditions at 180 °C with 0.5% of  $\text{H}_2\text{SO}_4$  as explained in the Experimental Section.

**Lignin Extraction.** The results of lignin extraction from beech wood are presented in Table 1. The reaction time was adjusted to account for the significantly faster reaction rates of the ether bond in GVL compared to GVL/ $\text{H}_2\text{O}$  observed using the conversion of the model compound BPE. Since almost all ether bonds were cleaved in the model compound after 120 min, the lignin extraction using GVL was performed for 30, 60, and 120 min, while in GVL/ $\text{H}_2\text{O}$ , the reaction time was prolonged to 120, 180, and 240 min.

After 120 min of treatment, a considerably lower amount of lignin was isolated using GVL (32.7%) in comparison to GVL/ $\text{H}_2\text{O}$  (51.1%). The lower amount of the isolated biopolymer in combination with the higher yield of residue points toward issues with lignin accessibility in the case of pure GVL. As discussed earlier, during the delignification of the LC biomass, lignin is released from the cellular and intercellular material because the ether bonds between the lignin fragments or in the lignin-carbohydrate complex are hydrolyzed.<sup>37</sup> In this particular case, the dissolution of lignin from the intercellular material was achieved while the release from the cellular material was suppressed due to the minor quantities of water in the system, namely, in 2 M  $\text{H}_2\text{SO}_4$  solution.

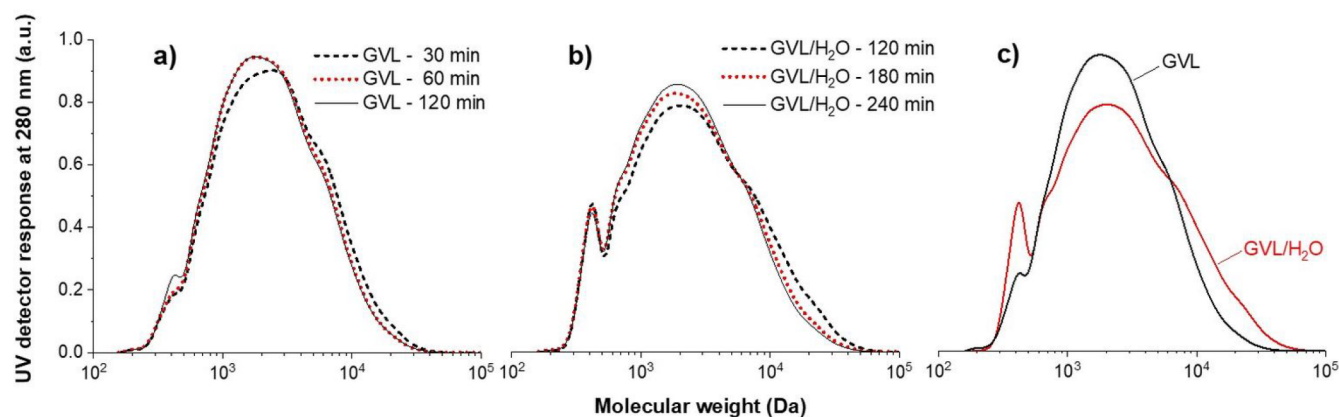


**Figure 4.** SEC chromatograms of lignin samples isolated using GVL for 30, 60, and 120 min (a); GVL/H<sub>2</sub>O for 120, 180, and 240 min (b); GVL for 120 min and GVL/H<sub>2</sub>O for 120 min (c).

Upon substituting 25 vol % of GVL with water, a significant difference is observed. The yield of recovered lignin increases with treatment time and reaches 65.7% after 240 min. Water evidently plays an important role by initiating hydrolysis of the ether bonds in the lignin–carbohydrate complex and within lignin itself, thus liberating biopolymer also from the cellular material.<sup>37</sup> Approximately 65% of lignin was recovered under the reaction conditions: 180 °C, 4 h, 0.019 M, GVL/water 3:1. The result is comparable with the data reported in the literature; for instance, the yield of lignin recovered by Jampa et al. was 41% (reaction conditions: 160 °C, 24 h, 0.22 M, GVL/water 4:1),<sup>15</sup> while nearly the same amount (40%) was isolated by Fang and Sixta (reaction conditions: 170 °C, 2 h, 0.05 M, GVL/water 9:1).<sup>16</sup> The comparison of the results suggests that the temperature and water amounts are the key parameters to improve the yield of lignin. This is also in agreement with the results obtained for the model compound BPE, which showed the importance of the temperature and the minor effect of acidity.

**SEC Analysis.** The apparent effect of both solvents on lignin is determined with an SEC analysis. The weight average molecular weight ( $M_w$ ) and number average molecular weight ( $M_n$ ) values for all lignin samples are listed in Table 1. The  $M_w$  of the GVL–lignin samples was in the range from 3750 to 3500 Da, while GVL/H<sub>2</sub>O lignins showed larger structures (4900–4200 Da). As expected from the experiments with BPE, due to the significantly faster ether bond cleavage in GVL compared to GVL/H<sub>2</sub>O, more depolymerized lignin macromolecules were isolated in nonaqueous solvent. While the average  $M_w$  remains nearly unchanged, a slight decrease in average  $M_n$  from 1530 to 1420 Da evidences a continuous, although minor lignin depolymerization. The gradual breakdown of the lignin network is clearly apparent in Figure 4a, where the intensity of the shoulder in the higher  $M_w$  region of the GVL–30 min lignin is reduced, while the intensity of the main peak in GVL–60 min lignin correspondingly increases indicating the formation of the larger amount of the smaller fragments. The occurrence of the shoulder in the low  $M_w$  region in the GVL–120 min lignin chromatogram additionally points toward the continuous lignin degradation and formation of the oligomeric structures.

Lignin depolymerization in GVL/H<sub>2</sub>O was consistent with the results obtained using BPE. The average  $M_w$  values decrease from 4900 to 4200 Da with increasing reaction time, clearly indicating the gradual simultaneous lignin isolation and depolymerization. In principle, a different lignin depolymeriza-

tion pathway can be inferred from the chromatogram profiles shown in Figure 4b. The average  $M_w$  consistently decreases with the reaction time analogously as during the GVL–lignin isolation, where the shoulder in the higher  $M_w$  region (sample GVL/H<sub>2</sub>O–120 min) is first reduced followed by a gradual increase of the main peak (sample GVL/H<sub>2</sub>O–180 and 240 min). The distinctive peak in the lower  $M_w$  region with a nearly constant intensity presumably represents smaller oligomeric lignin fragments that were formed after the ether bond cleavage and benzyl carbocation reaction with water.

Overall, by plotting chromatogram profiles of the GVL–120 min and GVL/H<sub>2</sub>O–120 min lignin samples shown in Figure 4c, the characteristic differences between the treatments become visible. The rate of the lignin depolymerization and the more pronounced formation of the oligomeric lignin fragments stand out.

**NMR Analysis.** Semiquantitative <sup>1</sup>H–<sup>13</sup>C HSQC and quantitative <sup>31</sup>P NMR analysis were employed to give the detailed structural and compositional information of different isolated lignin samples obtained in this study. The results of the 2D HSQC analyses are summarized in Figure 5. As expected, the catalytic activity of ether cleavage in pure GVL was repeatedly confirmed by estimating the content of the β-O-4 linkages (A) in GVL 30 min and GVL 120 min samples at δ<sub>C</sub> 73–77.5 and δ<sub>H</sub> 4.76–5.1 ppm. The hardly observable cross signal indicates that the majority of β-O-4 bonds were cleaved within the initial 30 min leaving only 1.13–1.129 per 100 C9 units, which persisted relatively unchanged during the remaining reaction time. The increase of the β-5 (B) and β-β (C) substructures from 2.44 to 2.91 per 100 C9 units and from 6.70 to 8.72 per 100 C9 units, respectively, points toward condensation reactions creating new C–C bonds within the aliphatic side chains. The emergence of the condensed structures is clearly shown by the appearance of the intensive cross signal at δ<sub>C</sub> 106–109 and δ<sub>H</sub> 6.35–6.65 ppm corresponding to the condensed syringyls (S<sub>condensed</sub>). Moreover, the strong cross signal at δ<sub>C</sub> 115–120.5 and δ<sub>H</sub> 6.48–7.06 ppm corresponding to the G<sub>5</sub> and condensed guaiacyls (G<sub>condensed</sub>) together with cross signals of significantly lower intensity relating to the G<sub>2</sub> (δ<sub>C</sub> 111.5–116; δ<sub>H</sub> 6.78–7.14 ppm) and G<sub>6</sub> (δ<sub>C</sub> 120.5–124.5; δ<sub>H</sub> 6.65–6.96 ppm) implies that the G units are also involved in the condensed lignin network formation.<sup>27</sup> In addition, it was observed that the S/G ratio decreased, suggesting the predominance of the simultaneous degradation of S units.



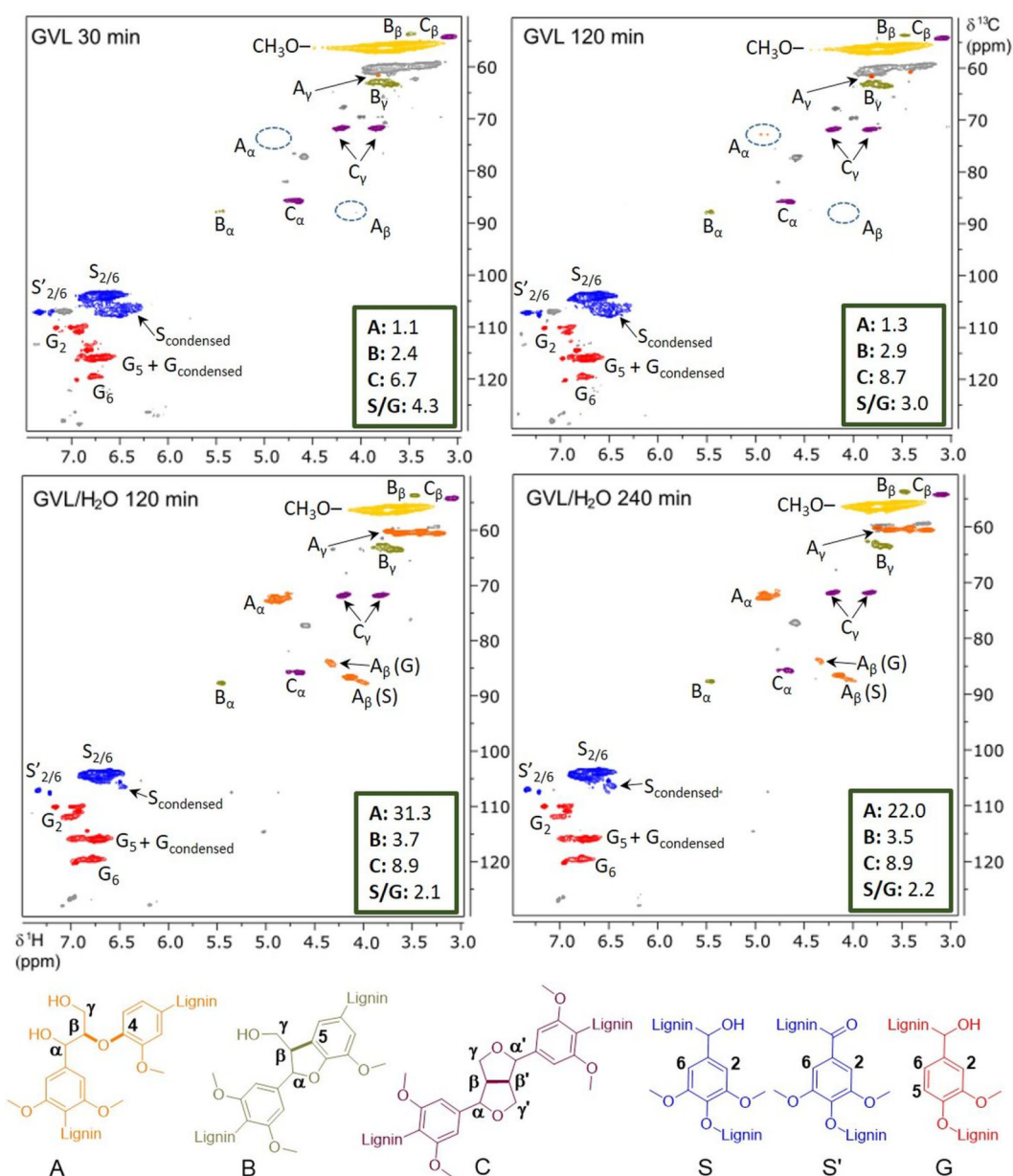


**Figure 5.** 2D HSQC NMR spectra and the major structures of lignins isolated in GVL and GVL/H<sub>2</sub>O: A, ( $\beta$ -O-4)  $\beta$ -aryl-ether units; B, ( $\beta$ -5) phenylcoumaran structures; C, ( $\beta$ - $\beta$ ) resinol structures; S, syringyl units; S', oxidized syringyl units; G, guaiacyl units. The amount of the major linkages is calculated per 100 C<sub>9</sub> units.

Completely different behavior was discovered once water was added to replace 25% of GVL as solvent. Lignin depolymerization over the  $\beta$ -O-4 bond cleavage was significantly slower, which is reflected in 31.3 per 100 C<sub>9</sub> units of preserved ether bonds in the GVL/H<sub>2</sub>O-120 min lignin sample. This value was reduced to 22.0 per 100 C<sub>9</sub> units within the subsequent pretreatment time (additional 120 min). Overall, the scission of the  $\beta$ -O-4 inter-unit linkage proceeds approximately 30 times faster in nonaqueous GVL. In contrast to the GVL-lignin, however, only negligible condensation reactions were observed within the aromatic units. In addition, the S/G ratio persisted nearly unchanged and correlated with the amount of the  $\beta$ - $\beta$  and  $\beta$ -5 linkages that were maintained approximately constant.

Quantitative <sup>31</sup>P NMR analysis is a well-known analytical technique developed for the determination of different OH

group content in lignin.<sup>45</sup> With this method, the change in the aliphatic and phenolic OH group content was examined at different reaction times, as shown in Figure 6. The total phenolic OH group content represents a cumulative value of the syringyl, guaiacyl, and *p*-hydroxyphenyl -OH groups.

The aliphatic OH group content in GVL 30 min lignin was determined to be 1.57 mmol g<sup>-1</sup> and persisted nearly unchanged, while only a minor increase of the phenolic OH group content from 2.25 mmol g<sup>-1</sup> to 2.48 mmol g<sup>-1</sup> was observed within the last 60 min of the reaction. The negligible changes in both aliphatic and phenolic OH group content within the first 60 min points toward a very rapid depolymerization of the accessible lignin. Simultaneous  $\beta$ -ether bond cleavage presumably followed by the guaiacyl unit substitution points rather to the molecular rearrangement than to the formation of the larger polymeric structures. This

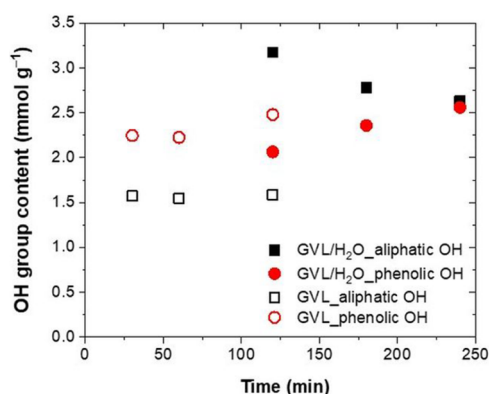


**Figure 6.** Phenolic and aliphatic OH group content in lignin isolated with GVL and in GVL/H<sub>2</sub>O with time.

interpretation could explain the ultimate increase in phenolic OH without notably changing  $M_w$ . The reduced S/G ratio (2D HSQC analysis) indicated the preferential degradation of the S units which in turn could generate lignin oligomers, detected as a newly emerged peak in the low  $M_w$  region (Figure 4a; GVL-120 min). Moreover, the elemental composition of the isolated lignin samples listed in Table 1 also supports the hypothesis about the molecular rearrangement within the lignin molecule as no changes were observed between the C, O, and H contents in GVL and GVL/H<sub>2</sub>O lignins. In addition, a lack of tendency to form larger polymeric structures, identified using BPE, could presumably be caused also by the steric hindrance of the neighboring functional groups; therefore new C–C bonds could rather be formed with G units as proposed in Scheme 2.

The addition of water significantly affects the isolation pathway and the structure of lignin. Our previous findings show that the ether bond cleavage in the presence of water is less intensive, resulting in an additional OH group. Consequently, the aliphatic OH group content in GVL/H<sub>2</sub>O-120 min lignin was determined to be 3.17 mmol g<sup>-1</sup>, which is twice as much as in GVL-lignin (1.57 mmol g<sup>-1</sup>). A subsequent decrease of the aliphatic OH group content to 2.63 mmol g<sup>-1</sup> during the next 120 min of the reaction and a simultaneous increase of the phenolic OH group content from 2.06 mmol g<sup>-1</sup> to 2.56 mmol g<sup>-1</sup> imply that the lignin depolymerization is preferred over the ether bond cleavage. Interestingly, GVL-120 min and GVL/H<sub>2</sub>O-240 min lignin have almost the same amount of the phenolic OH groups despite differences in the molecular weight and aliphatic OH group content.

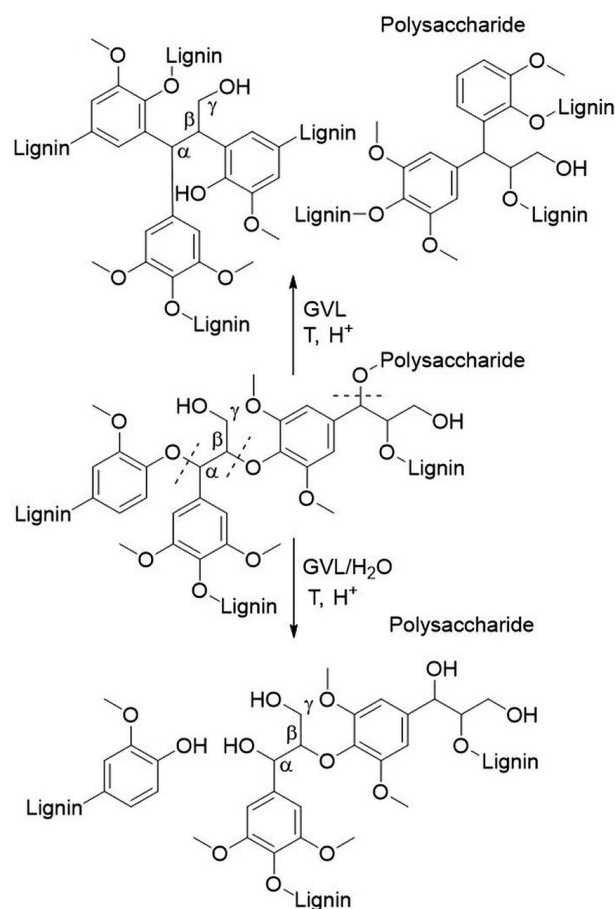
Overall, understanding the simultaneous lignin isolation and depolymerization along with the solvent effect during the biomass fractionation, the macromolecule with entirely different molecular weight and reactivity (functionality) and structure could be selectively obtained.

## CONCLUSIONS

To understand lignin chemistry, specifically the aryl-ether bond cleavage in acidified aqueous and nonaqueous  $\gamma$ -valerolactone (GVL), benzyl phenyl ether (BPE) was used as a  $\alpha$ -O-4 ether linkage model compound.

The  $\alpha$ -O-4 ether bond cleavage in the studied environment is proposed to follow the S<sub>N</sub>1 mechanism as a stable carbocation is formed. The product distribution is strongly affected by the presence of water as a cosolvent, while the

## Scheme 2. Mechanism of the $\alpha$ -Ether and $\beta$ -Ether Bond Cleavage in Lignin during Organosolv Pulping in GVL and GVL/Water



temperature and the acidity of the reaction media had a minor effect. The addition of water was found to be advantageous because it inhibits the formation of dimeric/trimeric structures and instead introduces reactive OH groups.

The effect of solvent was additionally investigated on the lignins isolated using (non-)aqueous GVL under moderate reaction conditions. The structural lignin changes were consistent with the results obtained from the BPE acidolysis. Specifically, a rapid ether bond cleavage, observed under nonaqueous conditions, was reflected in a more extensively depolymerized and rearranged lignin molecule with a significantly reduced aliphatic OH group content. On the other hand, in aqueous GVL, a gradual ether bond cleavage and almost a twice as high aliphatic OH group content and less depolymerized lignin structures were attained.

## ASSOCIATED CONTENT

### Supporting Information

The Supporting Information is available free of charge at <https://pubs.acs.org/doi/10.1021/acssuschemeng.0c06099>.

List of the used chemicals; list of the experiments with model compound (BPE); detailed experimental procedures with BPE; detailed description of GC-MS analysis; normalized product distribution during the BPE acidolysis in acidified  $\gamma$ -valerolactone (GVL) with 1% of H<sub>2</sub>SO<sub>4</sub> at the different temperatures (PDF)

## AUTHOR INFORMATION

## Corresponding Authors

Miha Grilc – Department of Catalysis and Chemical Reaction Engineering, National Institute of Chemistry, 1000 Ljubljana, Slovenia; [orcid.org/0000-0002-8255-647X](https://orcid.org/0000-0002-8255-647X); Email: [miha.grilc@ki.si](mailto:miha.grilc@ki.si)

Blaž Likozar – Department of Catalysis and Chemical Reaction Engineering, National Institute of Chemistry, 1000 Ljubljana, Slovenia; Email: [blaz.likozar@ki.si](mailto:blaz.likozar@ki.si)

## Authors

Edita Jasiukaitytė-Grojdek – Department of Catalysis and Chemical Reaction Engineering, National Institute of Chemistry, 1000 Ljubljana, Slovenia

Matej Huš – Department of Catalysis and Chemical Reaction Engineering, National Institute of Chemistry, 1000 Ljubljana, Slovenia; [orcid.org/0000-0002-8318-5121](https://orcid.org/0000-0002-8318-5121)

Complete contact information is available at:

<https://pubs.acs.org/10.1021/acssuschemeng.0c06099>

## Author Contributions

All authors have given approval to the final version of the manuscript.

## Notes

The authors declare no competing financial interest.

## ACKNOWLEDGMENTS

This research was funded by the Slovenian Research Agency (research core funding P2-0152, infrastructure core funding IO-0003 and research projects J2-2492 and J2-1723). The work was partially carried out within the RDI project Cel. Cycle: Potential of biomass for development of advanced materials and biobased products, which is cofinanced by the Republic of Slovenia, Ministry of Education, Science and Sport, and European Union through the European Regional Development Fund, 2016-2020. The authors also acknowledge the contribution of COST Action CA17128.

## REFERENCES

- (1) Mary, J.; Bidy, M. J.; Scarlata, C.; Kinchin, C. Chemicals from Biomass: A Market Assessment of Bioproducts with Near-Term Potential Chemicals from Biomass; *Technical Report NREL/TP-5100-65509*, March 2016, DOI: [10.2172/1244312](https://doi.org/10.2172/1244312).
- (2) Kunaver, M.; Jasiukaityte, E.; Čuk, N.; Guthrie, J. T. Liquefaction of wood, synthesis and characterization of liquefied wood polyester derivatives. *J. Appl. Polym. Sci.* **2010**, *115*, 1265–1271.
- (3) Sun, Z.; Fridrich, B.; De Santi, A.; Elangovan, S.; Barta, K. Bright Side of Lignin Depolymerization: Toward New Platform Chemicals. *Chem. Rev.* **2018**, *118*, 614–678.
- (4) Calvo-Flores, F. G.; Dobado, J. A. Lignin as Renewable Raw Material. *ChemSusChem* **2010**, *3*, 1227–1235.
- (5) Gillet, S.; Aguedo, M.; Petitjean, L.; Morais, A. R. C.; Da Costa Lopes, A. M.; Łukasik, R. M.; Anastas, P. T. Lignin Transformations for High Value Applications: Towards Targeted Modifications Using Green Chemistry. *Green Chem.* **2017**, *19*, 4200–4233.
- (6) Luterbacher, J. S.; Azarpira, A.; Motagamwala, A. H.; Lu, F.; Ralph, J.; Dumesic, J. A. Lignin Monomer Production Integrated into the  $\gamma$ -Valerolactone Sugar Platform. *Energy Environ. Sci.* **2015**, *8*, 2657–2663.
- (7) Shuai, L.; Amiri, M. T.; Questell-Santiago, Y. M.; Héroguel, F.; Li, Y.; Kim, H.; Meilan, R.; Chapple, C.; Ralph, J.; Luterbacher, J. S. Formaldehyde Stabilization Facilitates Lignin Monomer Production During Biomass Depolymerization. *Science* **2016**, *354*, 329–333.
- (8) Parsell, T.; Yohe, S.; Degenstein, J.; Jarrell, T.; Klein, I.; Gencer, E.; Hewetson, B.; Hurt, M.; Kim, J. I.; Choudhari, H.; Saha, B.; Meilan, R.; Mosier, N.; Ribeiro, F.; Delgass, W. N.; Chapple, C.; Kenttamaa, H. I.; Agrawal, R.; Abu-Omar, M. M. A Synergistic Biorefinery Based on Catalytic Conversion of Lignin Prior to Cellulose Starting from Lignocellulosic Biomass. *Green Chem.* **2015**, *17*, 1492–1499.
- (9) Luterbacher, J. S.; Rand, J. M.; Alonso, D. M.; Han, J.; Youngquist, J. T.; Maravelias, C. T.; Pfleger, B. F.; Dumesic, J. A. Nonenzymatic Sugar Production from Biomass Using Biomass-Derived  $\gamma$ -Valerolactone. *Science* **2014**, *343*, 277–280.
- (10) Horváth, I. T. Solvents From Nature. *Green Chem.* **2008**, *10*, 1024–1028.
- (11) Mehdi, H.; Fábos, V.; Tuba, R.; Bodor, A.; Míka, L. T.; Horváth, I. T. Integration of Homogeneous and Heterogeneous Catalytic Processes for a Multi-Step Conversion of Biomass: From Sucrose to Levulinic Acid,  $\gamma$ -Valerolactone, 1,4-Pentanediol, 2-Methyl-tetrahydrofuran, and Alkanes. *Top. Catal.* **2008**, *48*, 49–54.
- (12) Lê, H. Q.; Ma, Y.; Borrega, M.; Sixta, H. Wood Biorefinery Based on  $\gamma$ -Valerolactone/Water Fractionation. *Green Chem.* **2016**, *18*, 5466–5476.
- (13) Lê, H. Q.; Pokki, J.-P.; Borrega, M.; Uusi-Kyyny, P.; Alopaeus, V.; Sixta, H. Chemical Recovery of  $\gamma$ -Valerolactone/Water Biorefinery. *Ind. Eng. Chem. Res.* **2018**, *57*, 15147–15158.
- (14) Shuai, L.; Questell-Santiago, Y. M.; Luterbacher, J. S. A mild biomass pretreatment using  $\gamma$ -valerolactone for concentrated sugar production. *Green Chem.* **2016**, *18*, 937–943.
- (15) Jampa, S.; Puente-Urbina, A.; Ma, Z.; Wongkasemjit, S.; Luterbacher, J. S.; van Bokhoven, J. A. Optimization of Lignin Extraction from Pine Wood for Fast Pyrolysis by Using a  $\gamma$ -Valerolactone-Based Binary Solvent System. *ACS Sustainable Chem. Eng.* **2019**, *7* (4), 4058–4068.
- (16) Fang, W.; Sixta, H. Advanced Biorefinery based on the Fractionation of Biomass in  $\gamma$ -Valerolactone and Water. *ChemSusChem* **2015**, *8*, 73–76.
- (17) Mellmer, M. A.; Sener, C.; Gallo, J. M. R.; Luterbacher, J. S.; Alonso, D. M.; Dumesic, J. A. Solvent Effects in Acid-Catalyzed Biomass Conversion Reactions. *Angew. Chem., Int. Ed.* **2014**, *53*, 11872–11875.
- (18) Song, B.; Yu, Y.; Wu, H. Insights into Hydrothermal Decomposition of Cellobiose in Gamma-Valerolactone/Water Mixtures. *Ind. Eng. Chem. Res.* **2017**, *56*, 7957–7963.
- (19) Galkin, M. V.; Samec, J. S. M. Lignin Valorization through Catalytic Lignocellulose Fractionation: A Fundamental Platform for the Future Biorefinery. *ChemSusChem* **2016**, *9*, 1544–1558.
- (20) He, J.; Lu, L.; Zhao, C.; Mei, D.; Lercher, J. A. Mechanisms of Catalytic Cleavage of Benzyl Phenyl Ether in Aqueous and Apolar phases. *J. Catal.* **2014**, *311*, 41–51.
- (21) Roberts, V.; Fendt, S.; Lemonidou, A. A.; Li, X.; Lercher, J. A. Influence of Alkali Carbonates on Benzyl Phenyl Ether Cleavage Pathways in Superheated Water. *Appl. Catal., B* **2010**, *95*, 71–77.
- (22) Pelzer, A. W.; Sturgeon, M. R.; Yanez, A. J.; Chupka, G.; O'Brien, M. H.; Katahira, R.; Cortright, R. D.; Woods, L.; Beckham, G. T.; Broadbelt, L. J. Acidolysis of  $\alpha$ -O-4 Aryl-Ether Bonds in Lignin Model Compounds: a Modeling and Experimental Study. *ACS Sustainable Chem. Eng.* **2015**, *3*, 1339–1347.
- (23) Yokoyama, C.; Nishi, K.; Takahashi, S. Thermolysis of Benzyl Phenyl Ether in Subcritical and Supercritical Water, and Supercritical Methanol. *Sekiyu Gakkaishi* **1997**, *40*, 465–473.
- (24) Jin, S.; Xiao, Z.; Chen, X.; Wang, L.; Guo, J.; Zhang, M.; Liang, C. Cleavage of Lignin-Derived 4-O-5 Aryl Ethers Over Nickel Nanoparticles Supported on Niobic Acid-Activated Carbon Composites. *Ind. Eng. Chem. Res.* **2015**, *54*, 2302–2310.
- (25) Balakshin, M.; Capanema, E.; Gracz, H.; Chang, H.; Jameel, H. Quantification of Lignin-Carbohydrate Linkages With High-Resolution NMR Spectroscopy. *Planta* **2011**, *233*, 1097–1110.
- (26) Tran, F.; Lancefield, C. S.; Kamer, P. C. J.; Lebl, T.; Westwood, N. J. Selective Modification of the  $\beta$ - $\beta$  Linkage in DDQ-Treated Kraft

Lignin Analysed by 2D NMR spectroscopy. *Green Chem.* **2015**, *17*, 244–249.

(27) Zijlstra, D. S.; de Santi, A.; Oldenburger, B.; de Vries, J.; Barta, K.; Deuss, P. J. Extraction of Lignin with High  $\beta$ -O-4 Content by Mild Ethanol Extraction and Its Effect on the Depolymerization Yield. *J. Visualized Exp.* **2019**, *143*, 1–12.

(28) Meng, X.; Crestini, C.; Ben, H.; Hao, N.; Pu, Y.; Ragauskas, A. J.; Argyropoulos, D. S. Determination of Hydroxyl Groups in Biorefinery Resources via Quantitative  $^{31}\text{P}$  NMR Spectroscopy. *Nat. Protoc.* **2019**, *14*, 2627–2647.

(29) Jasiukaityte-Grojzdek, E.; Kunaver, M.; Crestini, C. Lignin Structural Changes During Liquefaction in Acidified Ethylene Glycol. *J. Wood Chem. Technol.* **2012**, *32*, 342–360.

(30) McDonough, T. J. The Chemistry of Organosolv Delignification. *Tappi J.* **1993**, *76*, 186–193.

(31) Sturgeon, M. R.; Kim, S.; Lawrence, K.; Paton, R. S.; Chmely, S. C.; Nimlos, M.; Foust, T. D.; Beckham, G. T. A Mechanistic Investigation of Acid-Catalyzed Cleavage of Aryl-Ether Linkages: Implications for Lignin Depolymerization in Acidic Environments. *ACS Sustainable Chem. Eng.* **2014**, *2*, 472–485.

(32) Elder, T.; del Río, J. C.; Ralph, R.; Rencoret, J.; Kim, H.; Beckham, G. T.; Crowley, M. F. Coupling and Reactions of Lignols and New Lignin Monomers: A Density Functional Theory Study. *ACS Sustainable Chem. Eng.* **2020**, *8*, 11033–11045.

(33) Sangha, A. K.; Parks, J. M.; Standaert, R. F.; Ziebell, A.; Davis, M.; Smith, J. C. Radical Coupling Reactions in Lignin Synthesis: A Density Functional Theory Study. *J. Phys. Chem. B* **2012**, *116*, 4760–4768.

(34) Pelzer, A. W.; Broadbelt, L. J. Effects of Substituents on the  $\text{S}_{\text{N}}2$  Free Energy of Activation for  $\alpha$ -O-4 Lignin Model Compounds. *J. Phys. Chem. C* **2017**, *121*, 7603–7614.

(35) Smit, A.; Huijgen, W. Effective Fractionation of Lignocellulose in Herbaceous Biomass and Hardwood Using a Mild Acetone Organosolv Process. *Green Chem.* **2017**, *19*, 5505–5514.

(36) Laure, S.; Leschinsky, M.; Fröhling, M.; Schultmann, F.; Unkelbach, G. Assessment of an Organosolv Lignocellulose Biorefinery Concept Based on a Material Flow Analysis of a Pilot Plant. *Cellul. Chem. Technol.* **2014**, *48*, 793–798.

(37) Lê, H. Q.; Zaitseva, A.; Pokki, J. P.; Ståhl, M.; Alopaeus, V.; Sixta, H. Solubility of Organosolv Lignin in  $\gamma$ -Valerolactone/Water Binary Mixtures. *ChemSusChem* **2016**, *9*, 2939–2947.

(38) da Costa Lopes, A. M.; Gomes, J. R. B.; Coutinho, J. A. P.; Silvestre, A. J. D. Novel Insights into Biomass Delignification With Acidic Deep Eutectic Solvents: a Mechanistic Study of  $\beta$ -O-4 Ether Bond Cleavage and the Role of the Halide Counterion in the Catalytic Performance. *Green Chem.* **2020**, *22*, 2474–2487.

(39) Frank, H. S.; Evans, M. W. Free Volume and Entropy in Condensed Systems III. Entropy in Binary Liquid Mixtures; Partial Molal Entropy in Dilute Solutions; Structure and Thermodynamics in Aqueous Electrolytes. *J. Chem. Phys.* **1945**, *13* (11), 507–532.

(40) Rezus, Y. L. A.; Bakker, H. J. Observation of Immobilized Water Molecules around Hydrophobic Groups. *Phys. Rev. Lett.* **2007**, *99*, 148301.

(41) Laage, D.; Stirnemann, G.; Hynes, J. T. Why Water Reorientation Slows without Iceberg Formation around Hydrophobic Solutes. *J. Phys. Chem. B* **2009**, *113*, 2428–2435.

(42) Galamba, N. Water's Structure around Hydrophobic Solutes and the Iceberg Model. *J. Phys. Chem. B* **2013**, *117*, 2153–2159.

(43) Southall, N. T.; Dill, K. A.; Haymet, A. D. J. A View of the Hydrophobic Effect. *J. Phys. Chem. B* **2002**, *106*, 521–533.

(44) Fengel, D.; Wegener, G. *Wood: Chemistry, Ultrastructure, Reactions*; Walter de Gruyter: New York, 2007, pp 26–59. DOI: 10.1515/9783110839654.

(45) Granata, A.; Argyropoulos, D. S. 2-Chloro-4,4,5,5-tetramethyl-1,3,2-dioxaphospholane, a Reagent for the Accurate Determination of the Uncondensed and Condensed Phenolic Moieties in Lignins. *J. Agric. Food Chem.* **1995**, *43*, 1538–1544.